MID-WAVELENGTH QUANTUM-WELL INFRARED PHOTODETECTORS

August 1998

M. Z. Tidrow, J. W. Little*, R. P. Leavitt, A. C. Goldberg*, and S. W. Kennerly
U.S. Army Research Laboratory
2800 Powder Mill Road
Adelphi, MD 20783

P. N. Uppal, and M. Sundaram
Sanders, A Lockheed Martin Company
65 Spit Brook Road
Nashua, NH 03061

**Also with the Univ. of Md., College Park, MD.*

ABSTRACT

Quantum-well infrared photodetectors (QWIPs) have developed rapidly over the past ten years. Most of the efforts have been concentrated on the long-wavelength and the very-long-wavelength regions of the thermal emission spectrum. Due to the success of InSb, HgCdTe, and PtSi detectors in the mid-wavelength infrared region, less emphasis has been placed on the development of QWIP focal-plane arrays operating in this wavelength band. However, recent interest in establishing pixel-registered, multispectral imaging capabilities has emphasized the need for high-quality mid-wavelength detectors that can be integrated with long-wavelength devices. In this presentation, the design and characterization of QWIPs using InGaAs/AlGaAs grown on GaAs substrates and InGaAs/InAlAs grown on InP substrates will be discussed. Both of these material systems can be used as single-wavelength, mid-wave devices and are compatible with vertical integration to give multispectral operation. Fundamental detector parameters, such as optical absorption strength, photoconductive gain, and temperature-dependent dark current, have been determined for various mid-wavelength QWIP designs and will be presented along with the results of single-pixel radiometric tests.

1.0 INTRODUCTION

The quantum-well infrared photodetector (QWIP) is a relatively new infrared (IR) device for focal-plane array (FPA) applications, compared with HgCdTe, InSb, PtSi, and extrinsic Si IR detectors. However, QWIP FPA technology using GaAs/AlGaAs on GaAs substrates has matured very quickly. Recently, large format FPAs with 640 x 480 elements that produce very

REPORT DOCUMENTATION PAGE

Form Approved OMB No. 0704-0188

1. REPORT DATE (DD-MM-YYYY)	2. REPORT TYPE	3. DATES COVERED (FROM - TO)
01-08-1998	Conference Proceedings	xx-xx-1998 to xx-xx-1998

4. TITLE AND SUBTITLE
Mid-Wavelength Quantum-Well Infrared Photodetectors
Unclassified

5a. CONTRACT NUMBER
5b. GRANT NUMBER
5c. PROGRAM ELEMENT NUMBER

6. AUTHOR(S)
Tidrow, M. Z. ;
Little, J. W. ;
Leavitt, R. P. ;
Goldberg, A. C. ;
Kennerly, S. W. ;

5d. PROJECT NUMBER
5e. TASK NUMBER
5f. WORK UNIT NUMBER

7. PERFORMING ORGANIZATION NAME AND ADDRESS
U.S. Army Research Laboratory
2800 Powder Mill Road
Adelphi, MD20783

8. PERFORMING ORGANIZATION REPORT NUMBER

9. SPONSORING/MONITORING AGENCY NAME AND ADDRESS
Director, CECOM RDEC
Night Vision and Electronic Sensors Directorate, Security Team
10221 Burbeck Road
Ft. Belvoir, VA22060-5806

10. SPONSOR/MONITOR'S ACRONYM(S)
11. SPONSOR/MONITOR'S REPORT NUMBER(S)

12. DISTRIBUTION/AVAILABILITY STATEMENT
APUBLIC RELEASE
,

13. SUPPLEMENTARY NOTES
See Also ADM201041, 1998 IRIS Proceedings on CD-ROM.

14. ABSTRACT
Quantum-well infrared photodetectors (QWIPs) have developed rapidly over the past ten years. Most of the efforts have been concentrated on the longwavelength and the very-long-wavelength regions of the thermal emission spectrum. Due to the success of InSb, HgCdTe, and PtSi detectors in the midwavelength infrared region, less emphasis has been placed on the development of QWIP focal-plane arrays operating in this wavelength band. However, recent interest in establishing pixel-registered, multispectral imaging capabilities has emphasized the need for high-quality mid-wavelength detectors that can be integrated with long-wavelength devices. In this presentation, the design and characterization of QWIPs using InGaAs/AlGaAs grown on GaAs substrates and InGaAs/InAlAs grown on InP substrates will be discussed. Both of these material systems can be used as single-wavelength, mid-wave devices and are compatible with vertical integration to give multispectral operation. Fundamental detector parameters, such as optical absorption strength, photoconductive gain, and temperature-dependent dark current, have been determined for various midwavelength QWIP designs and will be presented along with the results of singlepixel radiometric tests.

15. SUBJECT TERMS

16. SECURITY CLASSIFICATION OF:			17. LIMITATION OF ABSTRACT	18. NUMBER OF PAGES	19. NAME OF RESPONSIBLE PERSON
a. REPORT	b. ABSTRACT	c. THIS PAGE	Public Release	13	Fenster, Lynn lfenster@dtic.mil
Unclassified	Unclassified	Unclassified			19b. TELEPHONE NUMBER International Area Code Area Code Telephone Number 703767-9007 DSN 427-9007

high-quality imaging have been demonstrated.[1] However, most of the QWIP FPA development effort has concentrated on the long-wavelength IR (LWIR) region covering the atmospheric transmission window of 8 to 12 μm[1] and the very long wavelength IR (VLWIR) region (longer than 12 μm).[2] QWIPs have been demonstrated in the mid-wavelength IR (MWIR) band (i.e., the atmospheric transmission window of 3 to 5 μm),[3] but because of the maturity of existing MWIR materials systems such as InSb, HgCdTe, and PtSi, less emphasis has been placed on the development of MWIR QWIPs. In addition, the high aluminum concentrations required to obtain MWIR operation result in poor material quality in the standard GaAs/AlGaAs QWIP system. Therefore, new, less mature material systems are required for high-performance MWIR QWIPs.

Recent interest in establishing pixel-registered, multispectral imaging capabilities has emphasized the need for high-quality mid-wavelength detectors that can be integrated with long-wavelength devices. For example, a two-color (LWIR/MWIR) QWIP based on InGaAs/InAlAs grown on InP substrates is being developed under the U.S. Army's Multi-Domain Smart Sensors segment of Army Research Laboratory's Federated Laboratories program.[4] As part of this effort, new designs for MWIR QWIP, including coupled-quantum-well systems and advanced optical coupling structures, are being investigated to maximize detector performance in both wavelength bands. Programs of this type should lead to a new generation of MWIR QWIPs with performance that is competitive with currently available mid-wave systems.

2.0 INTERSUBBAND TRANSITIONS IN DOPED QUANTUM WELLS

Many conventional IR detector materials are narrow-bandgap semiconductors in which electron-hole pairs are generated by photons with energies at or above the bandgap of the material. The electron-hole pairs are swept by internal electric fields to contact layers where they are collected as a photocurrent. In contrast, QWIPs rely on an increase in the electrical conductivity that results when an absorbed photon excites an electron (or a hole) from a low-mobility bound state to a higher-mobility weakly bound state in a semiconductor quantum well. The wavelength of the absorbed photon is not determined by the bandgap of the materials but by the difference in bandgaps between the two materials that make up the quantum-well system. Therefore, materials such as GaAs and AlGaAs that are generally associated with near-infrared (~1 μm) devices can be used to make much longer-wavelength thermal detectors.

As shown in Figure 1, a quantum well consists of a thin layer of lower-bandgap semiconductor material such as GaAs surrounded by higher-bandgap layers such as AlGaAs. The discontinuity in the conduction band forms a potential-energy well for electrons in the lower-bandgap layer. For sufficiently thin wells (less than ~ 500 Å), the allowed energy levels are quantized into discrete subbands. Electrons (or holes) that populate the ground state (the lowest-energy subband) of the well (as the result of doping the well) can, under certain conditions, absorb a photon and undergo an intersubband transition[5] to a higher-energy excited state. The energy of the absorbed photon is equal to the difference in energy between the two subbands. The absorbed photon energy is determined by the width of the well, the magnitude of the potential-energy discontinuity (i.e., the depth of the well, determined by the compositions of the two layers), and the effective mass of the carrier in the well. The thickness, composition, and

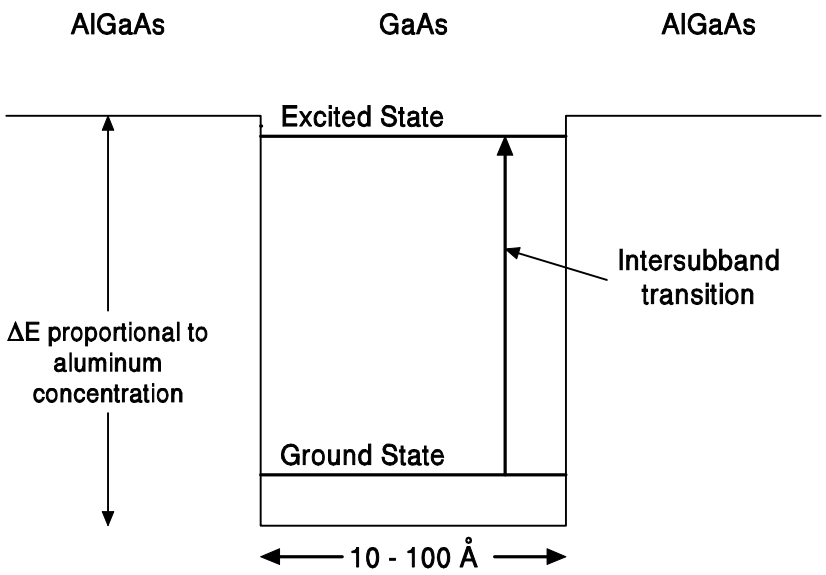

Figure 1. Energy-band diagram for a semiconductor quantum well.

doping of many III-V semiconductor materials can be precisely controlled using modern molecular beam epitaxy (MBE) growth techniques. Therefore, the intersubband transition in III-V semiconductor quantum wells can be designed to peak at a wide range of wavelengths, including those of interest for thermal imaging systems.

3.0 SEMICONDUCTOR MATERIALS FOR MWIR OPERATION

A typical GaAs/AlGaAs QWIP consists of 20 to 50 periods of the well/barrier layer combination shown in Figure 1, with doped contact layers above and below the quantum-well stack. For wider quantum wells, the excited state would be considerably below the conduction-band edge of the barrier and would be tightly bound to the well. However, here we show the excited state just below the top of the barrier where it is considered weakly bound to the quantum well. This configuration is typically used in the design of a QWIP so that electrons excited to the quasi-bound state as the result of the absorption of an infrared photon can easily tunnel through the triangular barrier formed when a small electric field is applied to the device (tilting the bands) and can travel through the barrier layer to be collected as a photocurrent. For narrower wells, the excited state would be unbound and would appear as a resonance above the top of the barrier.

The atomic lattice spacing of $Al_xGa_{1-x}As$ nearly matches that of GaAs for all values of x from 0 to 1. Therefore, for all aluminum compositions, this quantum-well system can be grown on a GaAs substrate with high crystal quality. Because the bandgap of $Al_xGa_{1-x}As$ increases monotonically with increasing aluminum mole fraction x, the depth of the well also increases with increasing x up to a maximum of about 910 meV (assuming that about 62% of the difference between the bandgaps of the barrier and the well appears in the conduction band).[6] For operation in the 3-to-5-µm wavelength band, the difference in energy between the subbands must be between about 250 meV (for 5-µm operation) to about 413 meV (for 3-µm operation). Therefore, for MWIR operation, the depth of the well must be on the order of 500 meV or larger.

While the GaAs/AlGaAs system appears to be ideal for this application (with well depths continuously variable up to about 900 meV), the maximum mole fraction that can be used for high-performance QWIPs is limited to about 0.40 (a 350 meV well depth), because above this mole fraction the material becomes indirect-gap, and the electron transport properties are seriously degraded by scattering into the low-mobility, indirect-gap valley and by the introduction of deep-level traps in the barrier layers.

If the height of the barrier is limited by material-quality considerations, the depth of the quantum well can be further increased by decreasing its bandgap. The ternary alloy $In_yGa_{1-y}As$ has a bandgap that decreases from that of GaAs monotonically with increasing indium mole fraction, y, and would therefore yield a deeper quantum well (for a given aluminum composition in the barrier layers). However, the atomic lattice spacing increases as the indium mole fraction is increased, so any InGaAs layer grown on a GaAs substrate is under compressive strain in the plane perpendicular to the growth direction. For sufficiently thin InGaAs layers (and sufficiently low indium mole fraction), this strain can be accommodated by elastic deformation of the lattice without the generation of dislocations in the crystal structure. We have found that, for well thicknesses typically used in QWIPs, indium mole fractions as high as 0.35 can be used without significant degradation of the crystal quality. When surrounded by barrier layers of $Al_{0.38}Ga_{0.62}As$, this composition gives a well depth of about 530 meV (when the effects of strain on the bandgap are accounted for). Therefore, this quantum-well system is appropriate for use in MWIR QWIPs as long as the total number of strained layers does not exceed a critical value after which dislocations are generated in the crystal.

Another promising semiconductor quantum well system consists of $In_{0.53}Ga_{0.47}As$ wells and $In_{0.52}Al_{0.48}As$ barriers. With the compositions given, both of the materials are lattice-matched to InP, which is a common substrate for MBE growth. Because this is an unstrained system, there is no restriction on the number of layers in the device. The well depth in this system is about 500 meV, which is appropriate for use in MWIR QWIPs.

Both of the alternative semiconductor systems described above can be used for LWIR/MWIR two-color detectors. A standard GaAs/AlGaAs LWIR design can be used with the strained InGaAs/AlGaAs MWIR QWIP. A wide InGaAs quantum well (lattice-matched to InP) can be used with InGaAs/InAlAs superlattice barriers in a miniband-transport (MBT) design to obtain LWIR operation.[4] Below, we discuss the minimum wavelengths and relative absorption strengths expected from these material systems and compare them with the standard GaAs/AlGaAs quantum well system.[4]

4.0 OPERATING WAVELENGTH AND ABSORPTION STRENGTH

The operating wavelength of a QWIP is determined by the difference between the energies of the ground state and the excited state of the quantum well. For an energy difference of ΔE, the peak wavelength, λ_p, is given by

$$\lambda_p = \frac{hc}{\Delta E} \quad , \tag{1}$$

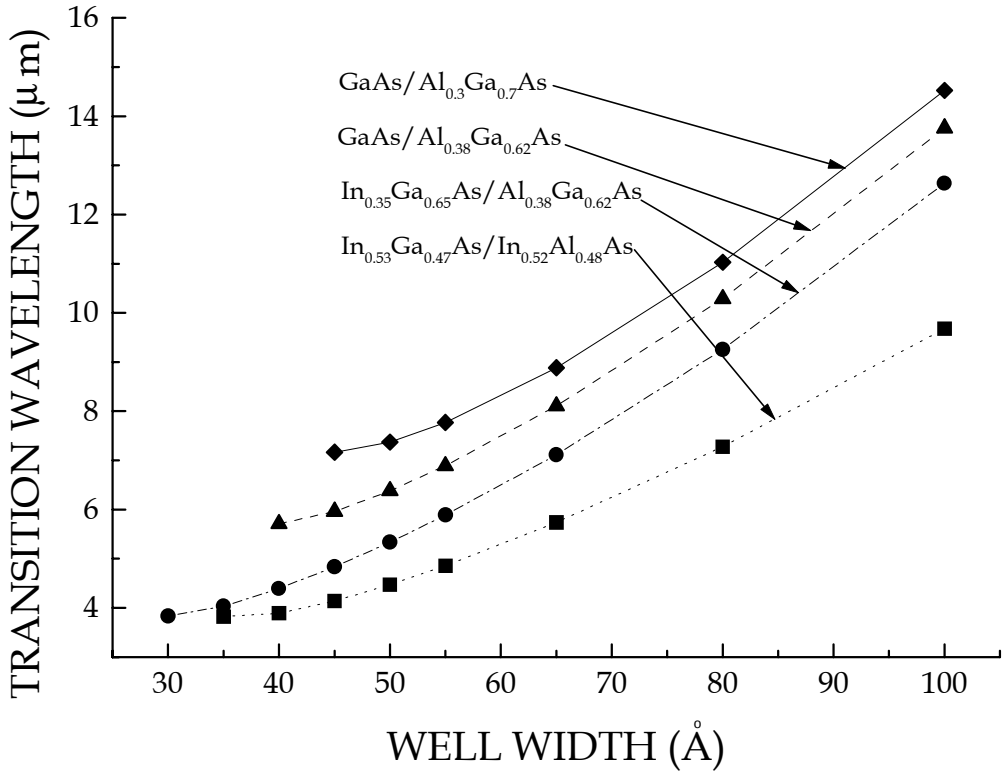

Figure 2. Intersubband transition wavelength versus well width for four quantum well systems.

where *h* is Planck's constant and *c* is the speed of light. The subband energies and the wave functions for different well/barrier compositions and well widths are calculated by solving Schrödinger's equation for an electron in the conduction band potential energy profile.

Figure 2 shows the peak wavelength vs. well width for four quantum-well systems. The first is for the $GaAs/Al_{0.3}Ga_{0.7}As$ system, which is used in LWIR MBT QWIPs and has provided excellent LWIR imaging. The second is for the $GaAs/Al_{0.38}Ga_{0.62}As$ system, which is close to the deepest-well system for direct-gap, unstrained layers on GaAs substrates. The third is for the $In_{0.35}Ga_{0.65}As/Al_{0.38}Ga_{0.62}As$ strained-layer system grown on GaAs. The fourth is for the $In_{0.53}Ga_{0.47}As/In_{0.52}Al_{0.48}As$ system grown on InP. The narrowest well width plotted for each system is the width corresponding to the minimum wavelength attainable for that system (i.e., the width for which the excited state becomes a resonant state above the barrier). Note that both indium-containing systems yield shorter minimum wavelengths (slightly less than 4 μm) than the GaAs/AlGaAs systems and are, therefore, better suited for MWIR operation.

The strength of the intersubband absorption depends on the number of electrons in the quantum well and the strength of the absorption for a single electron. This can be written as[7]

$$A = N_{2d}\ \sigma(E,\theta) \quad , \tag{2}$$

where A is the absorption per well, N_{2d} is the two-dimensional electron density in the well, and $\sigma(E,\theta)$ is the absorption cross section for a single electron in the quantum well. In general, the cross section depends on the energy of the photon (E) and the angle of incidence (θ) relative to the normal to the plane of the quantum well.

Fermi's golden rule can be used to calculate the transition rate, which, when divided by the photon flux, gives the cross section for absorption of the photon.[8] The infrared absorption cross section can be written as

$$\sigma(E) = \sigma_0 \sin^2\theta\ L(E) \quad , \tag{3}$$

where σ_0 is given by

$$\sigma_0 = \frac{4\pi^2}{137n} E_{fi} \left|\langle f|z|i\rangle\right|^2 \quad , \tag{4}$$

n is the index of refraction of the quantum well layers, E_{fi} is the energy difference between the final (excited) state and the initial (ground) state, and the absolute squared term is the dipole

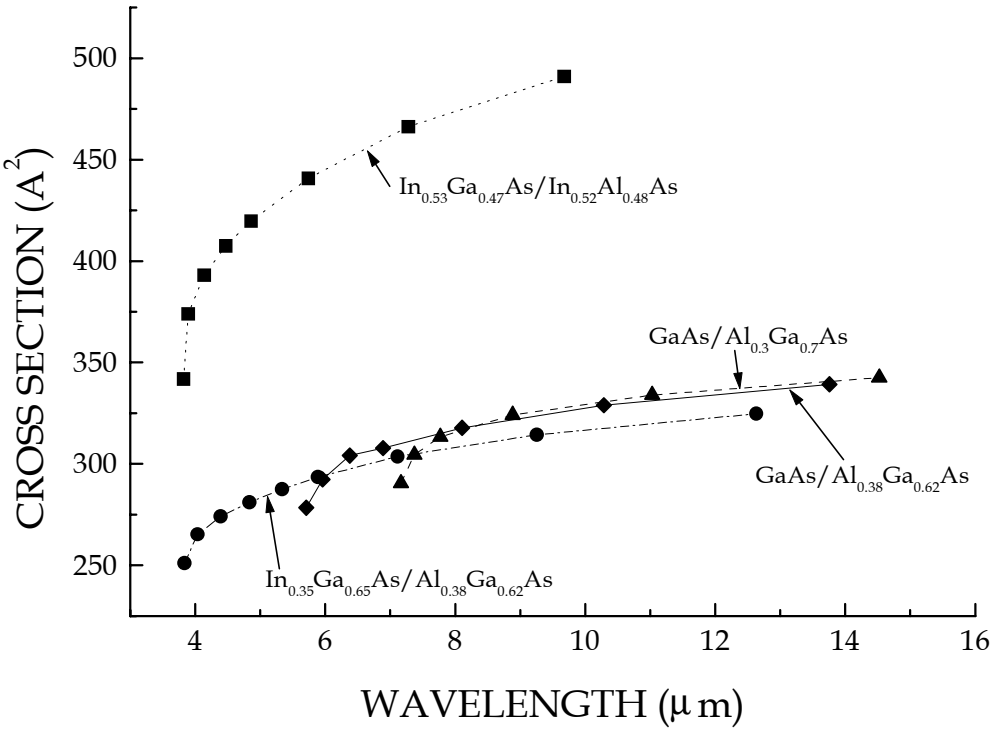

Figure 3. Absorption cross section versus transition wavelength for four quantum well systems.

matrix element between the final and initial state wave functions *f* and *i*, respectively. In equation 3, the term $L(E)$ is a normalized Lorentzian lineshape function given in terms of the full-width at half-maximum (FWHM), γ, by

$$L(E) = \frac{1}{\pi} \frac{\gamma/2}{(E - E_{fi})^2 + (\gamma/2)^2} \quad . \tag{5}$$

Figure 3 shows the maximum absorption cross section (equation 3 with $\theta = 90^o$ and the Lorentzian evaluated at the peak transition energy) for the four systems described above as functions of the operating wavelength. The FWHM was taken to be 8 meV, based on measurements made in our laboratory. Note that the calculated absorption strength for each material grown on GaAs substrates is about the same (for a given wavelength), while it is much larger for the InGaAs lattice-matched to InP. This is due primarily to the lower effective mass of the higher-indium-concentration, unstrained well material. In the strained-layer $In_{0.35}Ga_{0.65}As/Al_{0.38}Ga_{0.62}As$ system, the effects of strain tend to counteract the reduction in both the bandgap and the effective mass as compared with an unstrained layer of the same indium concentration.

These results show that the two indium-containing quantum-well systems can be used to make QWIP detectors with operating wavelengths of about 4 µm and absorption strengths about the same as or even larger than the standard GaAs/AlGaAs quantum wells. Preliminary results on MWIR QWIPs using these two quantum well systems are presented in the following sections.

5.0 $In_{0.35}Ga_{0.65}As/Al_{0.38}Ga_{0.62}As$ ON GaAs SUBSTRATES

The detector described here is part of a two-color QWIP consisting of two stacks of QWIPs for LWIR and MWIR detection.[9] The MWIR stack consists of 20 periods of 300-Å

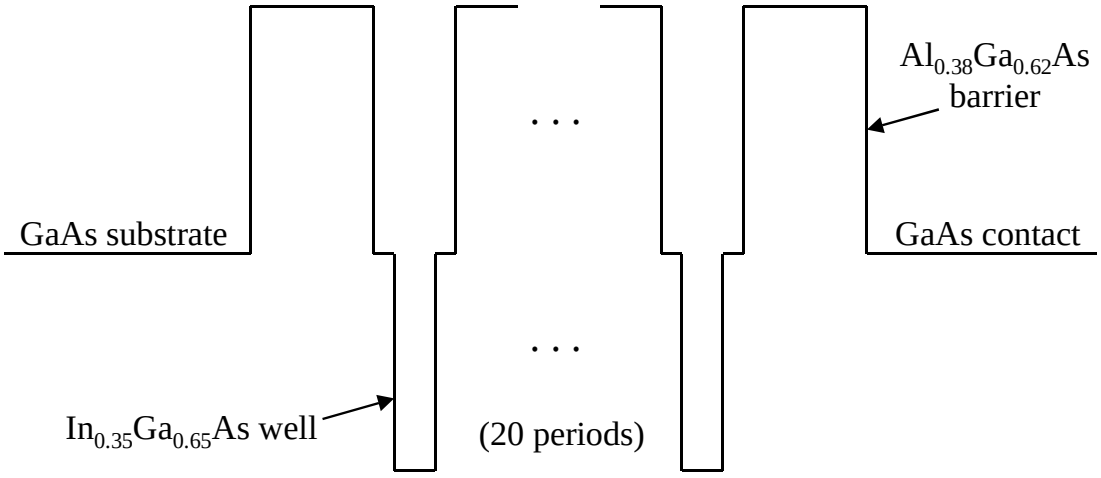

Figure 4. Two periods of a twenty-period strained-layer quantum well system (not to scale).

$Al_{0.38}Ga_{0.62}As$ barriers and 24-Å $In_{0.35}Ga_{0.65}As$ wells sandwiched between two 5-Å GaAs layers as shown in Figure 4. The doping concentration is 2.5 x 10^{18} cm^{-3} in the InGaAs quantum wells and is 1 x 10^{18} cm^{-3} in the contact layers. The sample was grown on semi-insulating GaAs (100) by MBE. Asymmetric (115) X-ray measurements showed a lattice relaxation of the in-plane lattice constant of less than 186 parts per million. The low dark current and the good uniformity of the device also show that the device is of high quality despite the high indium concentration.

The sample was processed into devices with mesa areas of 200 x 200 μm^2 using standard photolithography and wet chemical etching. A square ohmic contact ring composed of AuGe/Ni/Au was deposited on the periphery of the mesa and then alloyed for the ohmic contacts. A 45^o facet was polished on the side of the chip to allow for non-normal-incidence illumination of the mesas.

In the dark current and photocurrent measurements, the substrate contact was grounded, and positive or negative bias was applied to the top contact. Figure 5 shows the dark current for the MWIR stack measured at 77 K, 122 K, and 140 K, along with the 300-K window current measured at 30-K sample temperature with a field of view (FOV) of 180^o. The calculated window current at a 2-V bias is 3.95 x 10^{-5}A/cm^2, which is in excellent agreement with the measured values at 2-V bias. The background-limited infrared photodetector (BLIP) temperature was found to be 125 K up to ±2 V and 120 K up to ±3 V.

Photocurrent spectra were measured by front illumination using a monochromator and a calibrated glow-bar source. The IR radiation is incident normal to the 45^o facet. Figure 6 shows the peak responsivity vs. bias for the MWIR stack measured at 77 K. The responsivity spectrum

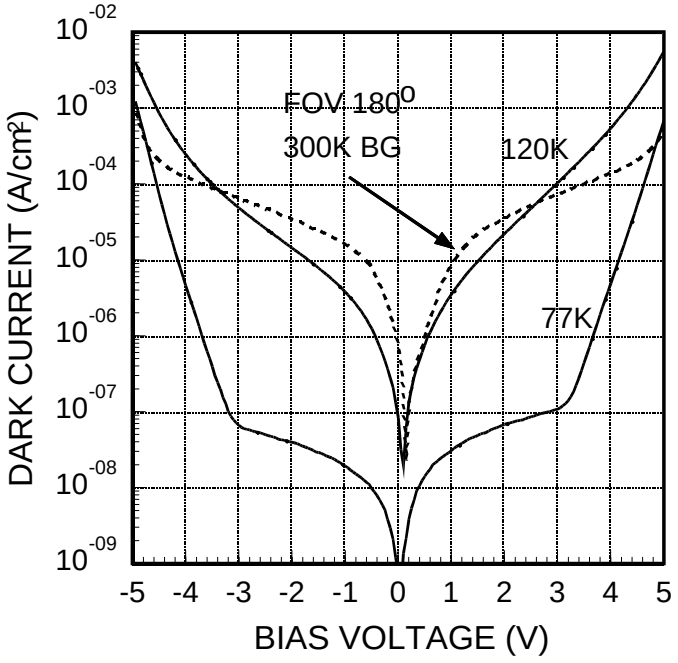

Figure 5. Dark current density of strained layer sample at 77 K and 120 K. Also shown is the 300-K background photocurrent with the sample at 30 K.

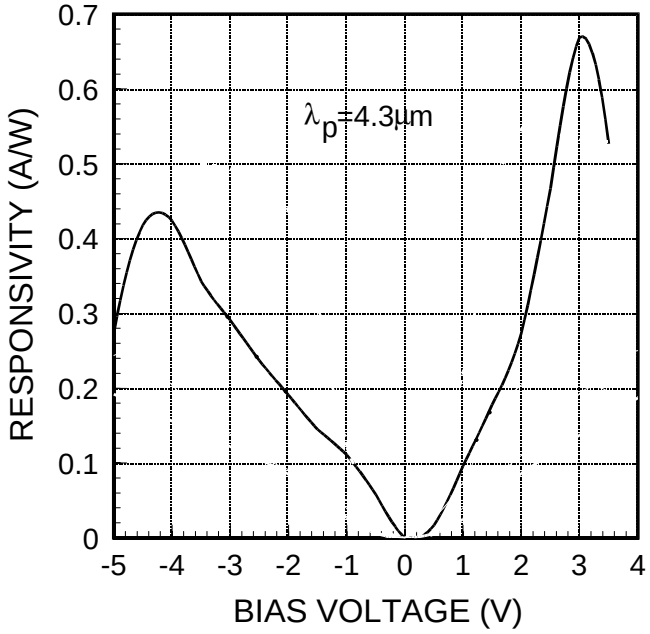

Figure 6. Peak responsivity versus bias for the strained-layer QWIP.

spectrum at 2 V is given in Figure 7 for the MWIR stack. The peak wavelength is at 4.3 μm with a maximum responsivity of 0.65 A/W at 3 V. At this bias, the cut-on wavelength (short-wavelength half-power point) is at 3.9 μm and cut-off wavelength (long-wavelength half-power point) is at 4.7 μm, which gives a FWHM of 0.8 μm. The MWIR stack is about 120 K BLIP at 3 V, and the BLIP spectral detectivity at 77 K is calculated to be D^*_{BLIP} =1.4 x 10^{11}cm-$Hz^{1/2}$/W assuming a 10% conversion efficiency.

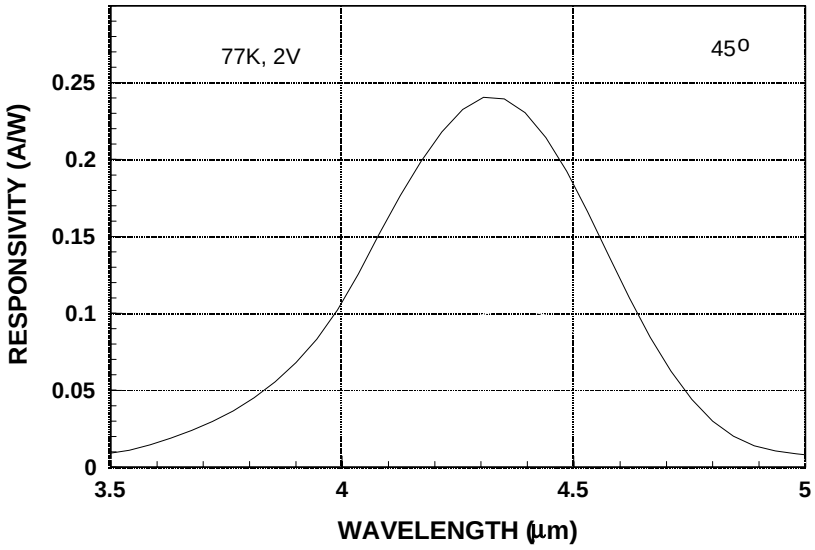

Figure 7. Spectral responsivity for the strained-layer QWIP.

6.0 $In_{0.53}Ga_{0.47}As/In_{0.52}Al_{0.48}As$ ON InP SUBSTRATES

This sample consists of 20 periods of 400-Å $In_{0.52}Al_{0.48}As$ barriers and 32-Å $In_{0.53}Ga_{0.47}As$ wells (n-doped to a level of 1 x 10^{18} cm^{-3}) grown on an InP substrate, with n-type contact layers above and below the quantum-well stack. A piece of the wafer was processed into 8 x 8 arrays of 100 x 100 μm^2 mesas using wet chemical etching. Au/Sn/Au contacts were deposited over the tops of the mesas and on the lower contact layer and annealed at about 360 °C for 30 s. A 45° facet was polished into the side of the chip, and the sample was mounted in a chip carrier with a 45° gold turning mirror in front of the polished facet to direct light into the facet parallel to the surface of the chip. This is a different illumination geometry than that used for the strained-layer sample described above, but the magnitude of the response measured in either way does not vary substantially. As for the previous sample, the lower contact was grounded, and the biases were applied to the top of the mesa.

The spectral response of this detector peaks at about 4.1 μm (at a bias of –3 V) with a FWHM of about 0.6 μm. Figure 8 shows the peak responsivity as measured using a chopped, 800-K blackbody IR source. The responsivity is about 0.34 A/W at –5-V bias and about 0.46 A/W at +5-V bias.

Figure 9 shows the current through the sample under several conditions. The lowest curve is for a 125-K sample temperature and a cold (80-K) background. The next curve is for a sample temperature of 125 K and an f/2.5, 300-K background. The current is slightly higher than that for a cold background, indicating that the sample is in a background-limited condition

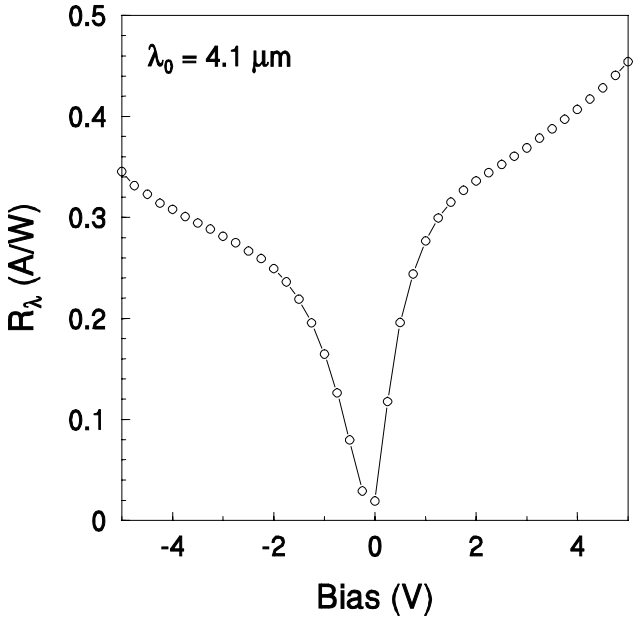

Figure 8. Peak responsivity versus bias for the unstrained quantum-well system

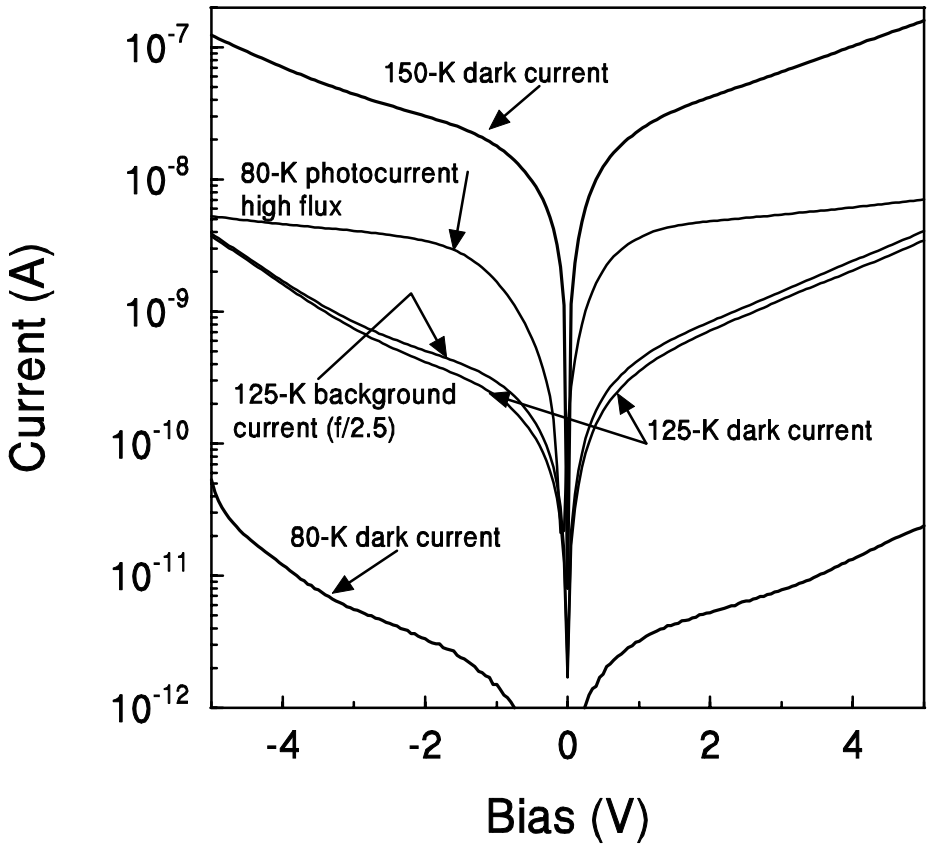

Figure 9. Current through unstrained sample for a variety of sample temperatures and illumination conditions. Note background-limited operation at 125-K sample temperature (f/2.5)

at 125 K for an f/2.5 room-temperature background. The next higher curve in Figure 9 is the current resulting from high-flux illumination of the sample at 80 K. The noise was measured under this condition (i.e., the majority of the current was photocurrent) and used to determine the photoconductive gain (by comparing the measured noise to the calculated shot noise for a given current). The top curve is for a 150-K sample temperature. The gain was also determined under this condition for which the current was dominated by thermally generated carriers. The two methods of determining the gain gave virtually the same values, and the results for the 150-K sample temperature case are shown in Figure 10. For absolute values of the bias greater than about 3 V, we believe that additional noise sources (other than shot noise) make the data invalid. Note, however, that for absolute biases between about 1.5 V and 3 V, the gain is greater than 1. These are preliminary measurements, and further study is required to ensure that this is an accurate determination of the gain in this system, and not just the result of spurious noise sources that are not properly accounted for.

Figure 11 shows the peak detectivity for 78-K, 125-K, and 150-K sample temperatures. For the two lower temperatures, the noise results from background photocurrent (and, therefore, the actual detectivities) are larger than the value of 4×10^{10} (cm$\sqrt{}$Hz/W) shown. For a 150-K sample

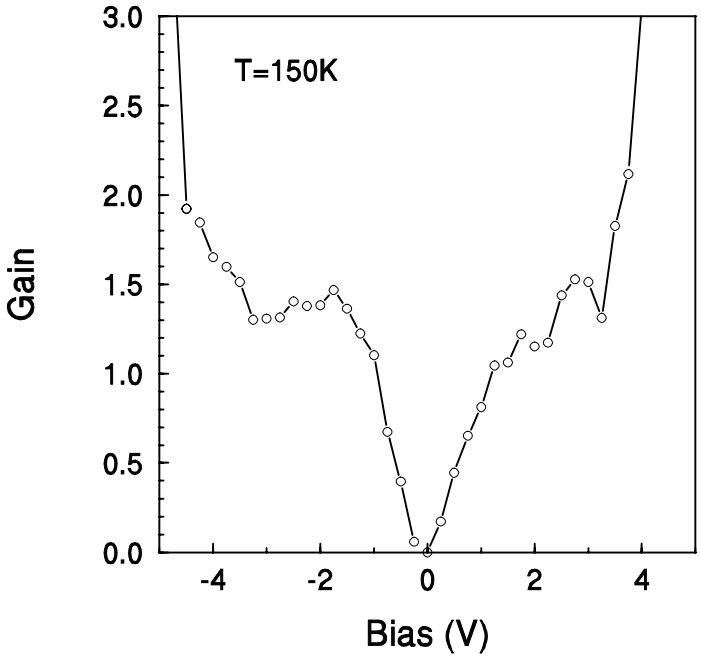

Figure 10. Photoconductive gain for unstrained QWIP measured at a sample temperature of 150 K.

temperature, the detectivity is on the order of 2 x 10^{10} (cm√Hz/W), which is good for a sample temperature this high.

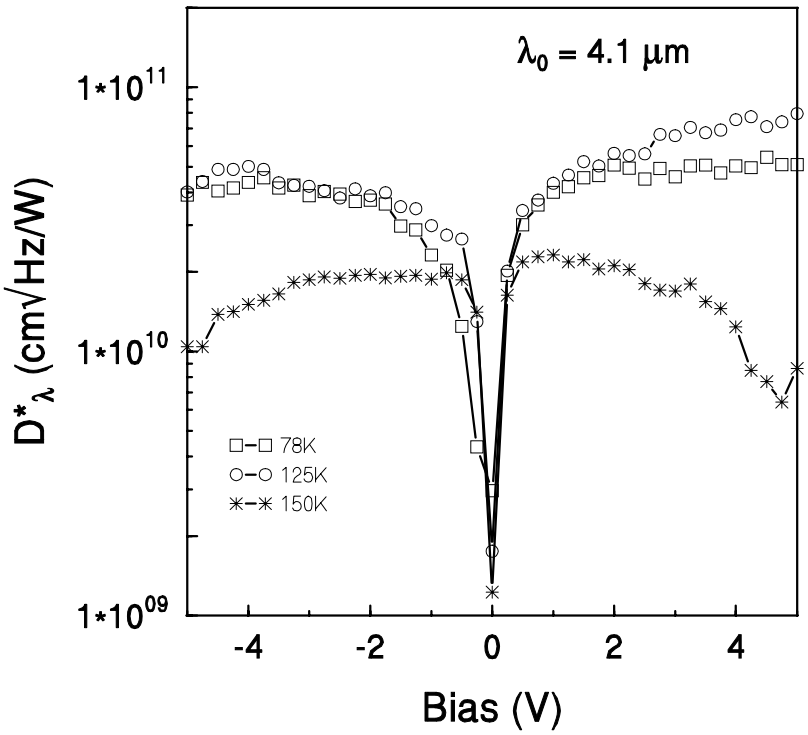

Figure 11. Detectivity for unstrained QWIP at sample temperatures of 78 K, 125 K, and 150 K.

7. SUMMARY

The ternary semiconductor alloy InGaAs, grown both as strained layers on GaAs substrates and unstrained layers on InP substrates, was shown theoretically to be a viable quantum-well material for use in MWIR QWIPs and multicolor FPAs. Detectors fabricated using both types of InGaAs quantum wells were shown to have high sensitivity and low dark current over a range of sample temperatures from 78 K to 150 K. Both types of QWIPs were background limited at about 125 K. Combined with the high-efficiency optical-coupling structures currently under development, these quantum-well material systems can be used in the fabrication of multicolor FPAs and in single-color MWIR FPAs with the potential for operation with thermoelectric coolers.

---

[1] W. A. Beck and T. S. Faska, SPIE Aerosense 1996, *Infrared Technology and Applications XXII*, Orlando, FL (1996); S. D. Gunapala, S. V. Bandara, J. K. Liu, W. Hong, M. Sundaram, R. Carralejo, C. A. Shott, P. D. Maker, and R. E. Muller, *SPIE Proceedings*, Orlando, FL (1997).

[2] S. D. Gunapala, J. K. Liu, M. Sundaram, S. V. Bandara, C. A. Shott, T. Hoelter, P. D. Maker, and R. E. Muller, *SPIE Proceedings*, Orlando, FL (1997).

[3] L. C. Lenchyshyn, H. C. Liu, M. Buchanan, and Z. R. Wasilewski, Semicond. Sci. Technol. **10**, 45 (1995).

[4] P. N. Uppal, R. P. Leavitt, J. W. Little, and S. W. Kennerly, Proceedings of the 1997 Sensors and Electron Devices Symposium, College Park, MD (1997).

[5] L. C. West and S. J. Eglash, Appl. Phys. Lett. **46**, 1156 (1985).

[6] G. W. Bryant, J. L. Bradshaw, R. P. Leavitt, M. S. Tobin, and J. T. Pham, Appl. Phys. Lett. **63**, 1357 (1993); J. L. Bradshaw, R. P. Leavitt, J. T. Pham, and F. J. Towner, Phys. Rev. B **49**, 1882 (1994).

[7] R. P. Leavitt, S. W. Kennerly, J. W. Little, D. W. Beekman, and A. C. Goldberg, *Proceedings of the 1998 Army Science Conference*, Norfolk, VA (1998).

[8] Edward. G. Harris, *Introduction to Modern Theoretical Physics*, Vol. 2, John Wiley & Sons, NewYork, (1975), pp. 586-588.

[9] M. Z. Tidrow, J. C. Chiang, Sheng S. Li, and K. Bacher, Appl. Phys. Lett. **70**, 859 (1997).